Journal of Radiological Protection

Official journal of the Society for Radiological Protection

PAPER

Numerical modelling of the transport and impact of ^{137}Cs and ^{131}I on the Meuse-Campine Canals after a potential nuclear accident

To cite this article: Amit Ravindra Patil *et al* 2025 *J. Radiol. Prot.* **45** 011512

IOP Publishing J. Radiol. Prot. 45 (2025) 011512 https://doi.org/10.1088/1361-6498/adc1db

Journal of Radiological Protection

PAPER

RECEIVED
29 November 2024

REVISED
11 March 2025

ACCEPTED FOR PUBLICATION
18 March 2025

PUBLISHED
27 March 2025

Numerical modelling of the transport and impact of ^{137}Cs and ^{131}I on the Meuse-Campine Canals after a potential nuclear accident

Amit Ravindra Patil[1,2,*], **Fabricio Fiengo Perez**[3], **Jonathan Lambrechts**[2] and **Eric Deleersnijder**[2,4]

[1] Belgian Nuclear Research Centre, Mol, Belgium
[2] Institute of Mechanics, Material and Civil Engineering, Université catholique de Louvain, Louvain-la-Neuve, Belgium
[3] Aquafin, Aartselaar, Belgium
[4] Earth and Life Institute, Université catholique de Louvain, Louvain-la-Neuve, Belgium
[*] Author to whom any correspondence should be addressed.

E-mail: amit.ravindra.patil@sckcen.be, fabricio.fiengo@aquafin.be, jonathan.lambrechts@uclouvain.be and eric.deleersnijder@uclouvain.be

Keywords: radiological impact assessment, Meuse River-Campine Canal, nuclear accident, radionuclide transport model, water ingestion doses

Supplementary material for this article is available online

Abstract

The Meuse River in Belgium can be impacted by the two nuclear power plants (Tihange and Chooz) located on its banks. Nuclear disasters such as the Fukushima and Chernobyl accidents have illustrated the risks associated with the civilian nuclear industry. In such situations, predictive models become crucial for developing environmental strategies to minimize the potential impact. In this study, we use the SLIM model to simulate the transport of ^{137}Cs and ^{131}I in the Meuse River system in Belgium. Several hypothetical accidental scenarios are considered for the radionuclide releases based on past nuclear accidents. The simulated radioactive distributions are then used to estimate the individual dose for drinking water. The radionuclide transport in the Meuse River is within days. While the higher peak concentration in the Meuse River results in higher individual dose. The Albert canal being the largest channel among the Campine canals; therefore, the radioactive plume stays over a month. The estimated individual doses for releases from Chooz Nuclear power plant near Tailfer reached 0.2 mSv within three days. Although it takes days, the doses in the Albert Canal reach values up to 0.46 mSv at Haccourt (hypothetical locations). The water extraction points in Herentals, located downstream of the canal, has a negligible individual dose estimation. Higher doses are the consequence of ^{131}I than ^{137}Cs due to the larger release scenario.

1. Introduction

Environmental emergencies, such as the contamination of a freshwater ecosystem following the release of radionuclides into the environment, will require strategies to minimize the negative impact of radioactivity (Hofman *et al* 2011). In this regard, numerical models are critical for predicting the behaviour of radionuclides in rivers and developing suitable plans for the management and remediation of contaminated areas (Monte *et al* 2005). After the Fukushima accident, the SPEEDI (System for Prediction of Environmental Emergency Dose Information) model results were not available for approximately two weeks; consequently, people were evacuated to areas with even higher concentrations due lack of precise information (Park *et al* 2017). Furthermore, high radioactivity concentrations were identified in tap water not just in Fukushima but also as far as Tokyo. Therefore, the International Atomic Energy Agency, in the wake of such nuclear accidents, have emphasized the need for numerical models (IAEA 2019) in order to make rapid decisions. Numerical models have proven to be useful not only in predicting the transport and fate of radionuclides but also as the basis for remediation (Zheleznyak *et al* 1992, Zheleznyak 1997, Siclet *et al* 2002, Monte *et al* 2009). Furthermore, such models can provide necessary information for dose assessment in the acute phase after a

severe nuclear accident before any intervention is possible (Simonsen *et al* 2019). This helps emergency responders take appropriate action while being informed about potential health risks.

During last two decades, numerical models have been developed to simulate radioactive dispersion in rivers (Monte *et al* 2005, 2006). However, the conceptualization of these models considered elements, such as tritium, technetium, iodine, and cesium, and thus, the predictions of these models have often ignored the interactions between radionuclides and solid matter (e.g. Behrens *et al* 2012, Estournel *et al* 2012, Tsumune *et al* 2012). This might be a reasonable simplification in short-term assessments, and for saving computational resources in accident cases when fast response is required (Duffa *et al* 2016).

In general, human activities rely significantly on waterways and have necessitated the construction of hydraulic structures to assure a continuous supply of drinking water and navigation. This in terms of water quality modelling requires additional considerations to accurately represent the radionuclide transport (Patil *et al* 2022). The Belgian Meuse River is one such unique navigation system, which is connected to a man-made canal system and features not one but two nuclear power stations (NPPs) on its banks. (figure 1). Indeed, these rivers are complex ecosystems with significant economic, social, and environmental value. Therefore, models that could be applied to simulate the dispersion of radionuclides released due to a potential accident occurring in either of the NPPs are rare in the literature.

Initial environmental risk assessments that have predictive characteristics use upper-bound predictions to account for the uncertainty (i.e. use of adequate safety margins). However, overly conservative predictions may raise unnecessary public concern. It is therefore important to obtain realistic worst-case (i.e. conservative) predictions that rely on process based models for radionuclide transport (Goulet *et al* 2022). For the Meuse River—Campine canal systems, due to lack of knowledge regarding the radioactivity dispersion, such radiological dose impact studies are also lacking. Here the estimated dose, which may be external or internal to the body can be used to identify potential risk associated to public health and thus safety guidelines can be developed (IAEA 2016) in the case of a nuclear emergency. Moreover, the dose assessment, even if it is less than the recommended value, will be crucial for monitoring public health for longer periods.

The purpose of the present paper is to fill the knowledge gap when describing the transport and fate of radionuclides in the Meuse River and its connected canal network (Campine canal). The two NPPs located on the banks are the Chooz NPP, which is in France near the border with Belgium, and the Tihange NPP, that is located near Amay in Belgium. The scenarios used in the present study for these NPPs were chosen to analyse the impact of a worst-case scenario. Here, the downstream flow of the river across these NPPs passes through many important cities, such as Namur, Liege, and Maastricht. Moreover, the connected canal networks can transport contaminants all the way to Antwerp. Since the Meuse River and the Albert Canal (the largest among the Campine Canal) are the primary sources of drinking water, the consequences of an accidental release into the river should be assessed. Therefore, in this study we also present the dose ingestion calculation for drinking water supply to evaluate the impact of such accidental scenarios. With this knowledge, suitable actions in terms of public health monitoring can be implemented.

The article is organized as follows. Section 2 starts by describing the flow characteristics of the Meuse River and the Campine Canal. Following that, a description of the model and the equations used to simulate the transport of radioactivity are presented. In addition, the conditions for hypothetical scenarios considered for a nuclear accident at Chooz and Tihange NPPs are given. In section 3, the simulated radionuclide distribution for accident scenarios in the river-canal system are presented, the arrival time, and the time when the activity levels are below the limit of 10 000 Bq m^{-3}. Later, the results of the temporal evaluation of individual doses at drinking water extraction locations are presented. Finally, a conclusion is given at the end of this article in section 4.

2. Materials and methods

2.1. Model domain

The Meuse River follows a transboundary course in Europe for up to 905 km in length (Beckers *et al* 2013). It originates in France and flows through Belgium to reach the North Sea through the Netherlands. The study area comprises the Meuse River in Belgium and the canal networks to which it is connected. The 143 km long stretch of the Meuse River considered here runs from the Belgian-French border to Maastricht in the Netherlands and is connected to the Albert Canal and the Zuid–Willemsvaart Canal. While the latter stretch over more than 46 km from Maastricht to Lozen, the former stretches more than 130 km from the Meuse River to the port of Antwerp. These two river-fed canals further distribute water into the smaller canals that are connected to one another. The study area thus includes a number of smaller canals, such as Bocholt–Herentals, Schoten–Dessel, Kwaadmechelen–Dessel, and Briegdan–Neerharn. These smaller canals

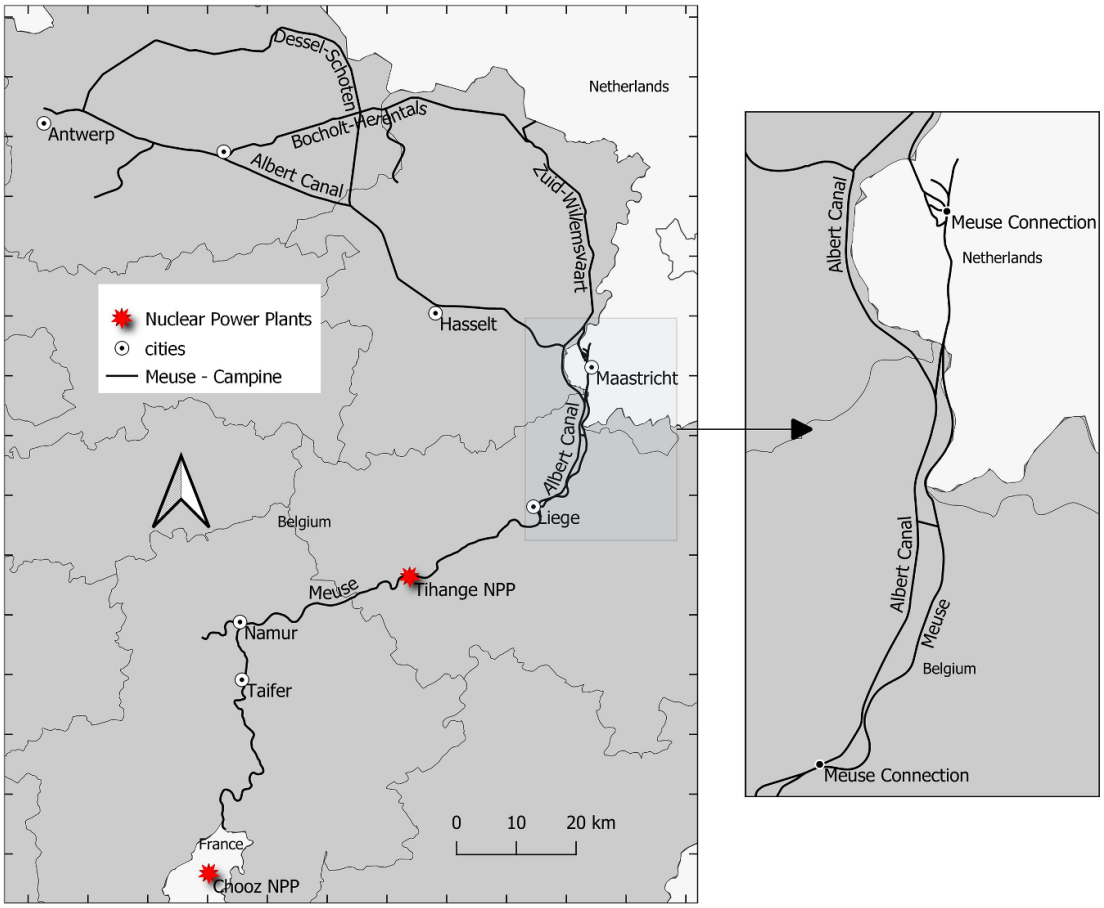

Figure 1. Course of the flow of Meuse River and its connection with the Campine Canals in Belgium: Location of the two NPPs located on the Bank of the Meuse River.

and the two river-fed canals together constitute the Campine canal. The domain of the study is shown in figure 1.

The Tihange and Chooz nuclear power plants are located in the upstream part of the Meuse River. The Tihange NPP is located in Huy on the right bank of the Meuse River and includes two active pressurized water reactors (PWR) with a combined capacity of 1992 MW. The Chooz NPP, located on the left bank at Belgian-French border, has two PWR with a combined net capacity of about 3 GW. In both NPPs, the river waters are used for cooling the reactors, of which 97% of the water used is returned to the river. Although, water discharges from nuclear power plants into the river contain some low-level radioactivity, the concentrations in the river water near the NPP are below the detection limits (FANC 2023).

2.1.1. Meuse river systems

The Belgian part of the Meuse River is highly regulated by a combination of weir systems and lock chambers, which play a major role in river flow dynamics. Along the Meuse River in Belgium, there are 15 weirs between French and the Netherlands border. These weirs raise the water level to obtain a sufficient hull for navigation, even during dry periods. For high flows, as the weirs are movable, they are operated to maintain the targeted water level in the river, thus preventing flooding. The regulation of these weirs is based on feedback from measuring stations. Furthermore, if the discharge in the river reaches a certain threshold, the target water level that needs to be maintained is lowered. This is done in order to prevent the weir directly upstream of the weir under consideration from becoming submerged. In specific locations, such as the weir at Liège (referred to as the Monsin Weir) located in the Meuse River just downstream the diversion with the Albert Canal (figure 1) controls the flow into the Albert Canal. A similar weir is also present in the river at the bifurcation of the Meuse at Maastricht. Upstream of this bifurcation on the left bank of the Meuse River, an underflow gate and lock chamber are used to feed water into the Zuid–Willemsvaart canal (figure 1) and to allow navigation through it.

The Albert and the Campine Canals comprise a total of 28 locks. Among them, the Albert Canal has six locks, each bounded at both ends by a set of three lock chambers. Navigation in this canal allows larger

vessels than in the other canals of the country. The smaller Campine canals, fed by the Zuid–Willemsvaart canal, are connected to the Albert Canal at four different places, as seen in figure 1. These canals are smaller in size, and navigation is made possible by a single lock chamber. Like the Meuse River, maintaining the water level in these canals is also of vital importance. For this purpose, there are bypass channels constructed across the lock chamber that allow the water to flow continuously once the target water level is reached. For the lock chamber placed in the other Campine Canals, the flow continuity is regulated by the culvert used for filling and emptying the lock chamber.

2.2. Model description

The water flow of the Meuse River and the Campine canal system is modelled here using the SLIM (Second generation Louvain-la-Neuve ice ocean model, www.slim-ocean.be) one-dimensional hydrodynamic model (Draoui *et al* 2020). The 1D model solves the Saint-Venant shallow water equation using the discontinuous Galerkin finite element method. Here, additional modules for incorporating the hydraulic structures are implemented to accurately describe the flow characteristics (flow cross-sectional area A and discharge Q) that are crucial in radionuclide transport purposes. Hourly discharges are prescribed at the upstream boundaries for the Meuse River and its tributaries. A full description of this model, including the details of numerical implementation and model validation against various measurements is given by (Patil *et al* 2022) and (Draoui *et al* 2020) for a thorough description of the methods used to implement the DG method for Saint–Venant equations used in the SLIM Model.

The radionuclides are simulated according to a Eulerian approach including advection, diffusion and decay at a constant rate. The corresponding equations are presented in equations (1) and (2):

$$\frac{\partial Ac}{\partial t} + \frac{\partial}{\partial x}(Qc) = \frac{\partial}{\partial x}\left(DA\frac{\partial c}{\partial x}\right) + S - \lambda Ac \tag{1}$$

$$\lambda = \frac{ln2}{T_{1/2}} \tag{2}$$

where, t is the time, D is the diffusion coefficient, c is the radionuclide concentration, S is the source for the radionuclide under consideration, λ is the decay constant, which is calculated in terms of the half-life ($T_{1/2}$) of the radionuclide. The source term S here is used to define radioactive fallout into the rivers or direct liquid releases. In the model, it is assumed that the radionuclides that enter the simulation domain are well mixed in the element where the release point is located. The composition of radionuclides considered in the release scenario is based on previous nuclear accidents (such as Fukushima), which have shown that ^{137}Cs and ^{131}I were among the primary radioactive substances that caused initial exposure to humans. Other processes, such as radionuclide adsorption to biological particles and suspended sediment, are excluded. This assumption is valid for accidental releases where the duration of the simulation period is short, or in the case of elements such as ^{131}I that do not tend to readily adsorb themselves to the sediments (Periáñez *et al* 2019).

Although regional authorities measure the radioactivity concentration in the river, the values are often below the detection limit. Moreover, the background radionuclides (from weapon testing and Chernobyl accidents) make it difficult to estimate the amount of concentration coming from the NPP directly. Due to the low activity levels the available information is not sufficient for the sake of validation. To the best of the author's knowledge, no other applicable measurement data exists for other types of pollutants. Therefore, the advection-diffusion transport equations here are verified with a classical approach by comparing them with analytical solutions. For this purpose, we consider point sources and Gaussian distributed sources with pure advection, diffusion, and a combination of advection-diffusion processes. Supplementary material shows the agreement between both the numerical and the exact solution. The model results show a good comparison with the exact solution to the problem.

2.2.1. Discussion on diffusion coefficient

The Advection-Diffusion-Decay equation (ADD) is implemented in tandem with the hydrodynamic model. The ADD equation requires defining the diffusion coefficient in order to represent the spreading of the pollutant. However, this coefficient needs to be defined either by using tracer experiments or by model calibration. Unfortunately, in this study, neither site specific nor activity concentration measurements were available for the selected rivers. Instead, we decided to base the values on empirical relationships that have been developed as a function of geometric and hydraulic parameters. These diffusion-induced dispersion equations will thus be based in the river's geometric features, such as the regularity of the river cross section and the width-to-depth ratio. Since the majority of the domain, in the Meuse River and traditionally the canal system is channelized, empirical relations suitable for this are chosen. Furthermore, a good precision is proven for rivers with a width-to-water depth (W/H) ratio of less than 100, this is the case for the aquatic

Table 1. Total radionuclide releases as reported by UNSCEAR from the Fukushima nuclear accident to the atmosphere release pathway into the aquatic environment.

Radionuclides	Atmospheric releases (PBq)
^{131}I	100–500
^{137}Cs	6–20

systems considered in this study (Zeng and Huai 2013). The empirical relationships used for the diffusion coefficients are represented in equation (3) (Iwasa and Aya 1991)

$$D_x = 2.0(W/H)^2 H u_* \tag{3}$$

where, D_x is the diffusion coefficient in longitudinal direction and u_* is the shear velocity.

2.3. Hypothetical scenario definition

2.3.1. Releases and source term definition

Here, we are interested in using this model to evaluate the impact of accidental releases coming from the Chooz and Tihange NPPs into the Meuse River. Several hypothetical accidents occurring in these two NPPs were considered and selected. These scenarios are selected in order to have worse-case conditions after atmospheric releases in the Meuse River systems. In previous nuclear accidents, such as the Fukushima disaster, this release pathway accounted for around 80% of the total contamination. The amount of radionuclide that is hypothetically released from both NPPs is based on the values from the Fukushima disaster by the UNSCEAR (United Nations Scientific Committee on the Effects of Atomic Radiation) (UNSCEAR 2021). Table 1 gives a description of the releases that were reported to occur during the Fukushima accident:

For the atmospheric deposition source, the JRODOS atmospheric model (Raskob *et al* 2016) was used to determine the distribution of both the radionuclides and their activities on the surface of the Meuse River. The JRODOS has been previously utilized for assessments following the Fukushima Daiichi accident (Ievdin *et al* 2012, Kovalets *et al* 2014, Selivanova *et al* 2023). For this study, the radioactivity deposition results were obtained with a release of 100 PBq in the case of ^{131}I and 10 PBq for the ^{137}Cs, assuming a release period of 6 h. The release period is assumed based on observations, which show that most of the peak release is achieved within this period of time. In the case of the Fukushima disaster, the hydrogen explosions that occurred on 12 March 2011, led to peak activity concentrations in the atmosphere being detected within hours (Tsuruta *et al* 2014).

2.3.2. Meteorological conditions of the study area

The river discharge has significant temporal variability in its flow that can influence the time scale and the distribution of radionuclide in these systems. During a year, the summer periods bring less precipitation, resulting in low discharges of around 50 $m^3\ s^{-1}$ and in wet winter periods, higher discharges up to 3000 $m^3\ s^{-1}$ can be observed (Ward *et al* 2008). Low discharges in the summer period can persist for a longer time, whereas high discharges usually reach a peak and subside as the precipitation reduces (figure 2). For our purposes, we take into account two scenarios with realistic flow conditions: First, is the low flow scenario and the other is high flow scenario (peak flows). Figure 2 shows a hydrograph of the Meuse River for the year 2013 and the flow scenario selected in this study. The high flow scenario peaks at 1025 $m^3\ s^{-1}$, while the low flow scenario reaches a minimum of 40 $m^3\ s^{-1}$ with an average flow of 54 $m^3\ s^{-1}$ over 42 d. Although the peak and the low flow periods in the Meuse River could vary between years, the aim here is to distinguish between the impact of low and high flows conditions on radioactivity distribution. In this preceptive, the selected scenarios could be considered as average scenarios for the Meuse River. The recurrence of peak flow (near Maastricht) is usually higher than 800 $m^3\ s^{-1}$ and it lasts roughly 25 d, for discharges above 1300 $m^3\ s^{-1}$, the occurrence of such event is around 165 d (Ward *et al* 2008).

In order to obtain a contamination event with maximum affected area and highest deposited activity, a constant wind speed of 1 m s^{-1} is chosen for both the NPPs, and a uniform and fixed direction of wind is chosen to be such that the released plume into the atmosphere is deposited towards the Meuse River basin. Figure 3 shows the area deposition of radionuclides, and table 2 presents the parameters used for the scenarios. It should be noted that in figure 3, the colourmap is limited to 7 MBq m^{-2} for both radionuclides.

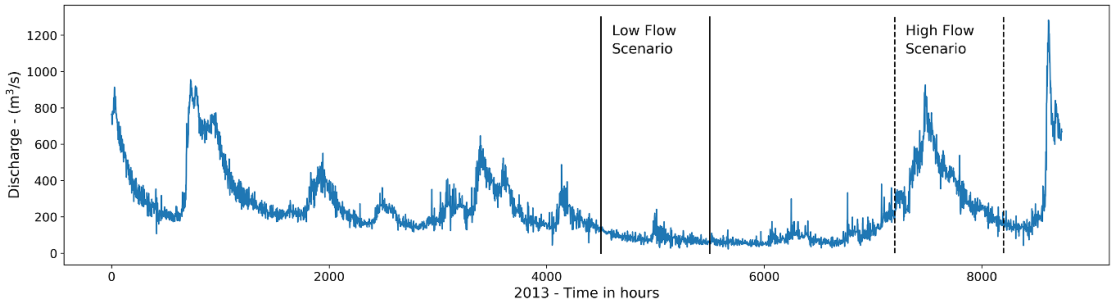

Figure 2. Hydrograph in Meuse River at Tihange NPP (2013): period of flow in the Meuse River considered for the scenarios in this study.

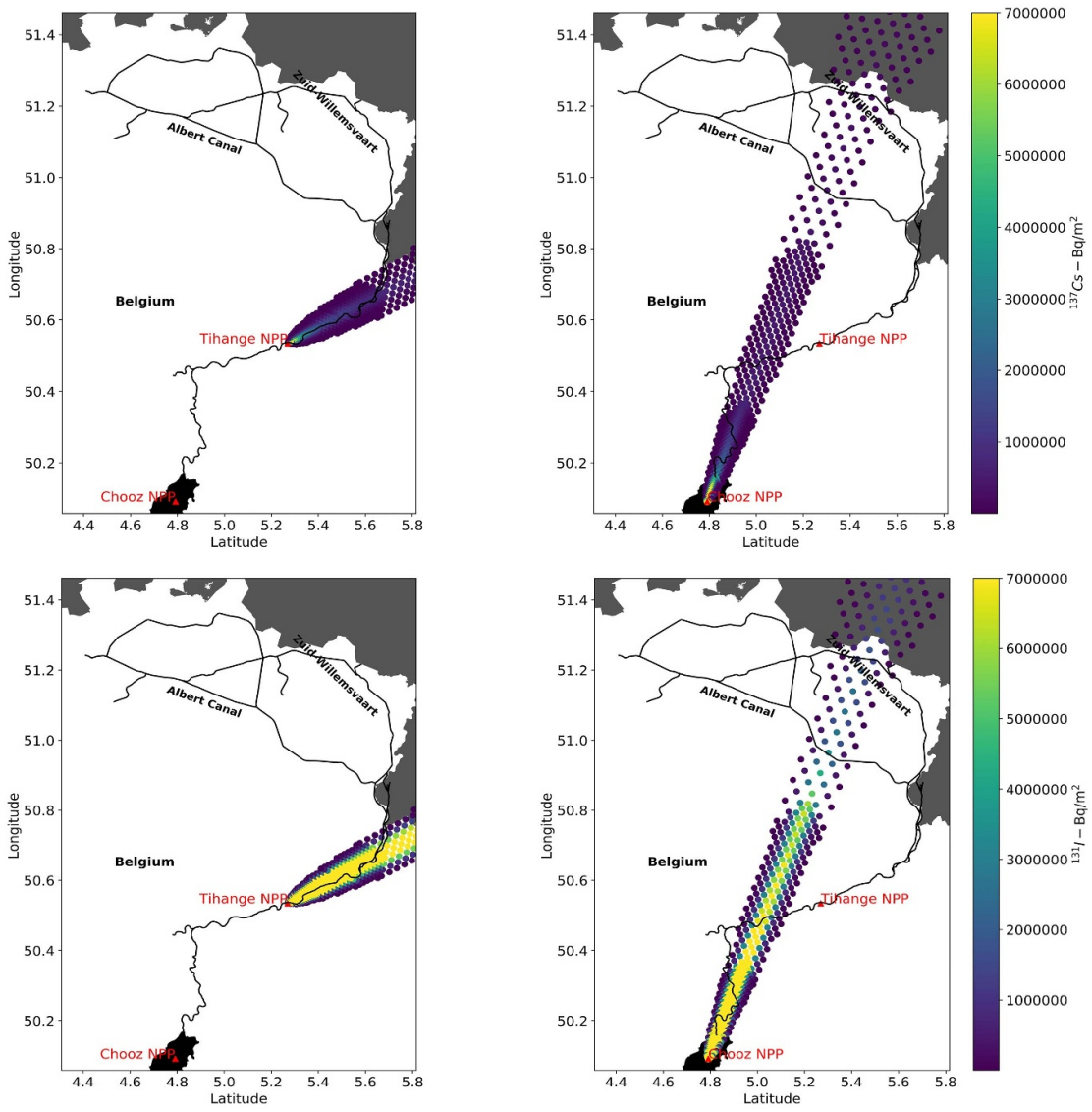

Figure 3. Total amount of radionuclide deposited on the Scheldt basin after 24 h of initial release as computed by the JRODOS model for ^{137}Cs and ^{131}I from Tihange NPP (left) and Chooz NPP (right).

2.4. Dose calculation for drinking water

In order to obtain the cumulative individual dose, the radioactivity concentration is multiplied by the dose coefficient for internal exposure via ingestion (internal dose rate)

$$\mathrm{Dose}_k\,(mSv) = A_k \times B \times \sum_t c_k \tag{4}$$

Table 2. Scenario definitions for ^{137}Cs and ^{131}I and their amount of radioactivity released from the NPPs (Tihange and Chooz) into the Meuse basin for the model.

Scenario	NPP	Radionuclide	Amount released	Direction (wind-blown from the source)
1	Tihange	^{137}Cs	10 PBq	56°
2		^{131}I	100 PBq	56°
3	Chooz	^{137}Cs	10 PBq	11°
4		^{131}I	100 PBq	11°

where k identifies the radionuclide, A_k is the dose coefficient for radionuclide k (mSv Bq^{-1}), B is the daily consumption of drinking water per person (lit/d), t is the number of days after the accident (consumption date), and c_k is the concentration of radionuclide k in drinking water at t hours after the accident. In this study, B was set at 2 lit/day, which is the IAEA's recommended value for dose estimation (IAEA 2016). The dose coefficients of 4.9×10^{-11} for ^{137}Cs and 7.4×10^{-10} Sv/Bq for ^{131}I are used (ICRP 2020). The assessment is based on the two water extractions carried out in the study area: (1) the Meuse River (extracted at Tailfer), which supplies drinking water to the Brussels region with a population of approximately 2 million people, and (2) the Albert Canal (extracted at Herentals), which provides 40% of total drinking water to a population of 7 million people in Flanders. Figure 4 shows the location of these water extraction points. Additionally, the total population dose is calculated by multiplying the dose and the total population that consumes the contaminated water. This is done to determine the carcinogenic likelihood for the population.

3. Results and discussion

3.1. Scenario Simulation: Activity concentrations in water

This section presents the radioactivity concentrations for the scenarios that were previously discussed in section 2.3. The radioactivity concentrations are evaluated using the recommended limit of 10 kBq m^{-3} (derived from the 0.1 mSv year^{-1} permissible dose according to the safety regulations under normal operating conditions) instead of absolute zero. However, it should be noted that these limits can be modified based on the level of accident and are typically much higher (IAEA 2016). Figure 4 shows some of the important locations used in this section to show the temporal variation of the radionuclide activity. Sections 3.1.1 and 3.1.2 compare the results of Tihange NPP releases, whereas section 3.1.3 shows the results of Chooz NPP.

3.1.1. High vs low flow

The radionuclide takes about 8 h to deposit on the river, following which it gets transported to the downstream region of the river and the Campine canal. The distribution of radioactivity in these aquatic systems depends on the flow conditions of the river. Figure 5 shows the concentration of ^{137}Cs for both high and low flow scenarios (as described in section 2.3.2) after approximately 4 d of initial release (i.e. 100 h).

As shown in figure 5, in the initial days after the release, the affected areas of the radionuclide in the Campine canal are approximately similar. The maximum concentration at this hour for the case of high flow is 99 kBq m^{-3} located in the Meuse River, while that for low flow is 180 kBq m^{-3} located in the Albert Canal, closer to the river-canal confluence. Furthermore, figure 5 shows near to zero radioactive contamination in the Meuse River in the high-flow scenario. This is because the high flow scenario in the Meuse River reduces the flushing time from six to two days (see table 3). In contrast, the longer flushing time in the Albert Canal is due to the operation of hydraulic structures at the confluence (river—canal). This also applies to the other connection from the river to the Zuid–Willemsvaart canal, where the water discharge is controlled by an underflow gate.

However, the radioactivity distribution changes significantly for low and high flow scenarios in the canal systems. Figure 6 shows the radionuclide distribution after approximately 25 d of simulation.

Figure 6 shows that in the high flow scenario, the radioactive plume has reached Antwerp, whereas in the low flow scenario, it has only been transported until Genk (for location, see figure 4). Furthermore, unlike the high flow scenario, the radioactive plume that is transported along the Zuid–Willemsvaart canal reaches the downstream section of the Albert Canal earlier than the radioactivity plume that travels along the Albert Canal itself. This is illustrated in figure 7, which shows the concentration profile along the Albert Canal at the time the plume arrives from the connecting canals. In the low flow scenario (figure 7(a)), the radioactivity spike near Kwaadmechelan and Herentals, is visible while the plume in the Albert Canal continue to move towards it. For high flow scenario, the plume coming from the Zuid–Willemsvaart and its connecting canals

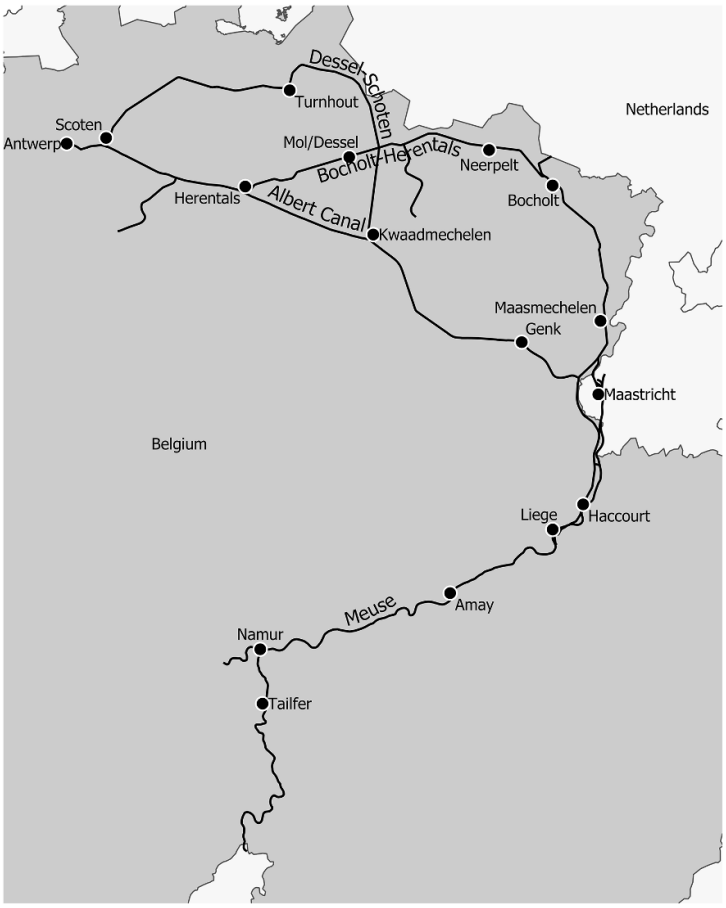

Figure 4. Location of important places used for estimating the residence time and dose calculation presented in this section.

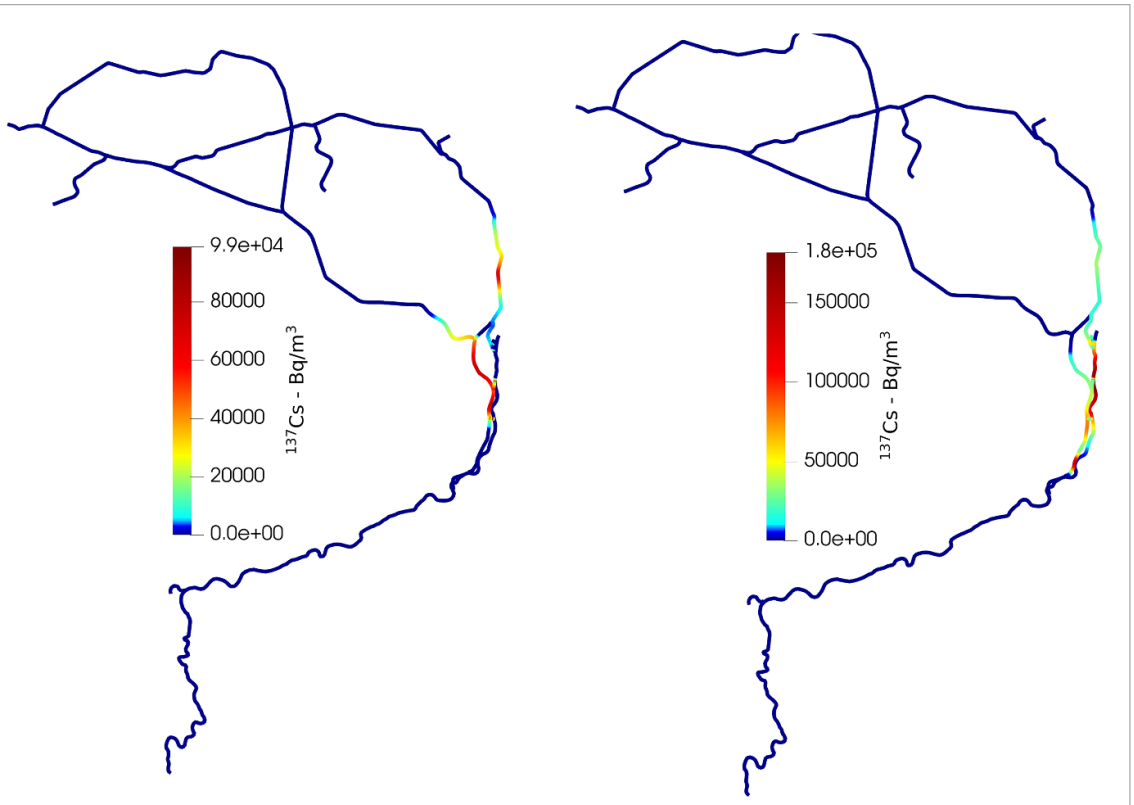

Figure 5. ^{137}Cs distribution in the Meuse—Campine Canal after 100 h of initial release for high flow scenario (left) and low flow scenario (right).

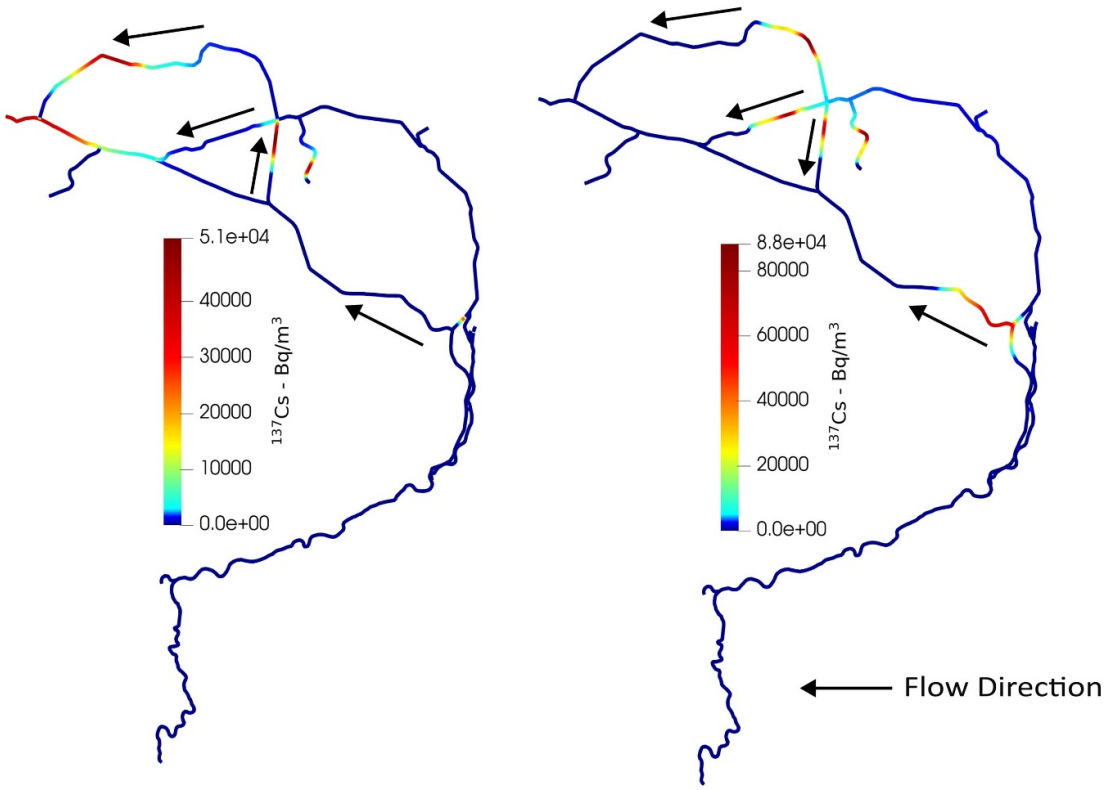

Figure 6. ^{137}Cs distribution in the Meuse—Campine Canal after 600 h of initial release (a) for high flow scenario (left) and (b) low flow scenario (right).

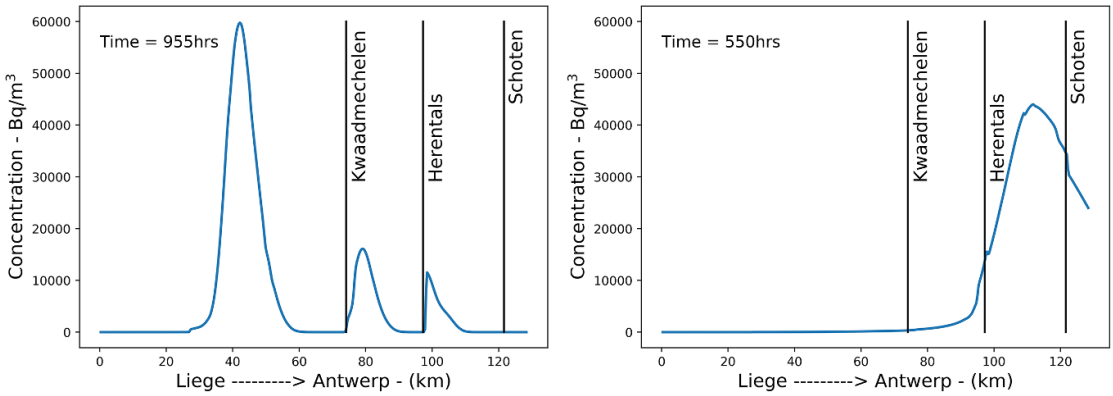

Figure 7. ^{137}Cs longitudinal profile along the Albert Canal from Liege to Antwerp for (a) Low flow scenario at 955 h (left) and (b) High flow scenario at 560 h after initial release (right).

coincides with the arrival of plume from the Albert canal (as illustrated in figure 7(b)). The slower transport of the plume in the Albert Canal (175 m wide in Genk) can be partially explained by its larger size compared to the other canals (42 m wide in Neerpelt). In addition to that, during low flows in the Meuse River, discharge diversion into the Albert Canal is lower than during the high flows.

Figure 6(a) further shows that the plume is still present in the Dessel–Kwaadmechelen Canal. This is due to the fact that during high flow in the Albert canal there is a shift in flow direction into the Dessel–Kwaadmechelen Canal. Moreover, during low flows the velocities in this segment are rather low. The Dessel–Kwaadmechelen Canal connects the Albert–Canal and the Bocholt–Herentals canal without any regulation in between its ends. Therefore, the direction highly depends on difference in water level between its both ends. During high flow events in the Albert Canal the plume in this canal segment will be flushed to the north, while during low flows it will slowly travel to the Albert Canal. This illustrates that the plume in the Albert Canal has the potential to re-contaminate the smaller Campine canals after the initial plume is transported.

Table 3. Arrival and End time of the potential plume in Meuse River and the network of Campine canal at specific location with maximum concentration and time of occurrence at that location.

Scenario	Canal name	City name	Arrival time (h)	End time (h)	Maximum conc. (kBq m^{-3})	Time for max conc.
Low flow	Meuse River	Maastricht	20	148	166	115
	Albert Canal	Genk	497	—	60.8	842
	Albert Canal	Antwerp	—	—	—	—
	Dessel–Schoten	Turnhout	683	859	83	794
	Dessel–Herentals	Mol	452	630	79.8	558
	Zuid–Willemsvaart	Maasmechelen	61	204	120	160
High flow	Meuse River	Maastricht	14	61	142	48
	Albert Canal	Genk	128	277	64	220
	Albert Canal	Antwerp	525	668	39	595
	Dessel–Schoten	Turnhout	460	545	47	504
	Dessel–Herentals	Mol	664	944	22	774
	Zuid–Willemsvaart	Maasmechelen	53	110	73	89

Table 3 shows the arrival, the end time from the initial release and the maximum concentration of the radionuclides at locations inside each of the canals (for location, see figure 4). It should be noted that the arrival and end times are estimated in terms of when the concentration reaches either below or above 10 000 Bq m^{-3}.

From the arrival/end times in table 3, it can be seen that the radionuclide contamination stays longer at a specific location during low flows than in the high flow scenario. For example, in Turnhout, the duration of the high contamination period for the release during the low flow scenario is 91 h (∼4 d) longer than if released during the high flow scenario. Similarly in the Meuse River, the plume stays for 81 h (∼3 d) longer in the case of a low flow scenario. This relatively lower period of contamination in the river than the canal can be related to the fact that the river's water velocities are high. Additionally, due to lower velocities in the canal the effect of diffusion increases. In most of the locations, the magnitude and time for peak concentration also decrease from low flow scenario to the high flow scenario except at Mol. The change in time of peak concentration at Mol is a result of the shift in flow direction in high flow from the low flow scenario in the Dessel–Kwaadmechelen canal. This dilutes the radioactivity from the Zuid–Willemsvaart canal, but also introduces radioactive contaminants from the Albert Canal at a later time.

For the Zuid–Willemsvaart canal, the peak concentrations at Maasmechelen in the low flow scenario are higher than those obtained during high flow scenario (table 3). Since the water in Brigeden–Nerhaaran canal is nearly stagnant, the radioactive plume in Zuid–Willemsvaart canal is mostly derived from the Meuse River. Figure 8 shows the distribution of radioactivity at the connection between the Zuid–Willemsvaart canal and the Meuse River in Maastricht after about 4 d of release. The period of maximum activity concentration at Maasmechelen (12 km from Maastricht) is 57 h in high flow, i.e. 10 h longer than at Maastricht (in Meuse River) and 143 h in low flow, i.e. 15 h longer. The longer times in the canal can be attributed to its slower velocities.

3.1.2. ^{131}I distribution

As described earlier for ^{137}Cs, the low flow scenario is typically the scenario for maximum impact in the Meuse River and the Campine canal. Therefore, the results for ^{131}I presented here are only for the low flow scenario. It is worth mentioning that the half-life of ^{137}Cs (30 years) is significantly longer than ^{131}I (8 d). However, the amount of ^{131}I that is released in the scenario is 10 times larger than the release of ^{137}Cs. Figure 9 shows the radionuclide distribution for ^{131}I after approximately 4 and 28 d of initial release.

Because of the high amount of ^{131}I released, the radioactive contamination is greater than ^{137}Cs after 4 d of the release. Furthermore, figure 9(a) shows that the peak concentration (∼7.9 MBq m^{-3}) is one order of magnitude higher than ^{137}Cs. However, since ^{131}I has a faster decay rate, the concentration in the system reduces significantly. Moreover, in the case of the Campine canal, since the concentrations are smaller than in the Albert Canal the radioactivity concentration vanishes (approximately 10 times smaller than the initial value) after about 20–27 d (figure 9(b)). However, for the high flow scenario, it is seen that the plume reaches Antwerp faster than the plume of ^{137}Cs. This is due to the considerably larger magnitude of the release of ^{131}I. Figure 10 shows the concentrations for both radionuclides along the Albert Canal at different times and flow scenarios.

Figure 10(a) shows the radionuclide distribution of ^{131}I and ^{137}Cs, where it can be seen that both plumes arrive at same time. However, nearly 28 d after the beginning of the release, the activity concentration of ^{131}I

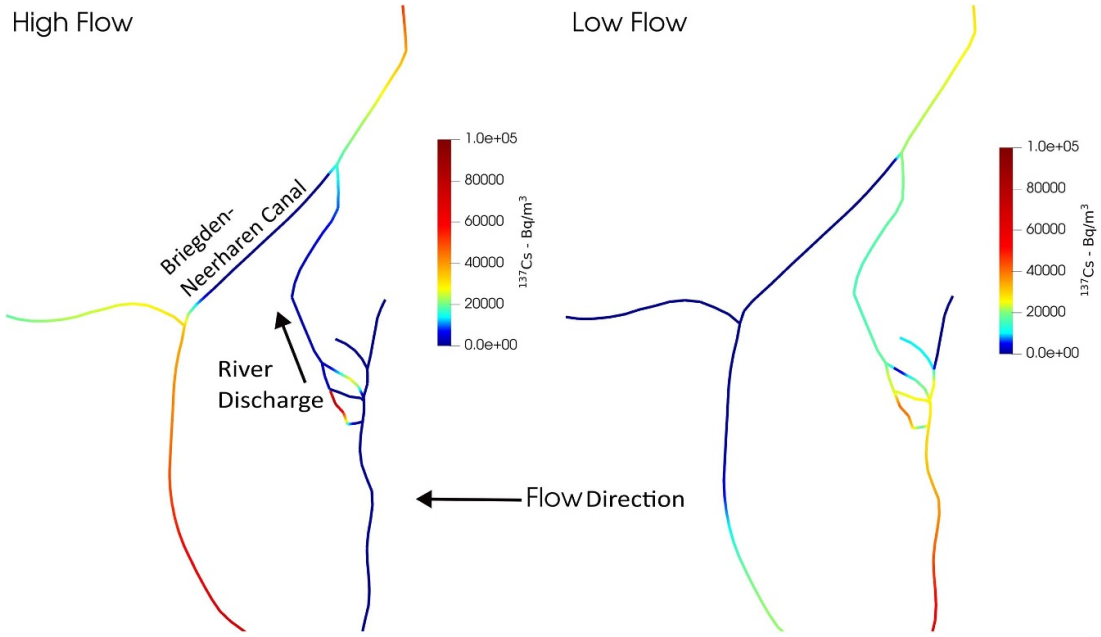

Figure 8. ^{137}Cs distribution at the connection of the Meuse River and the Zuid Willemsvaart canal (a) for high flow scenario at 100 h after initial release (left) (b) for low flow scenario at 100 h after initial release (right).

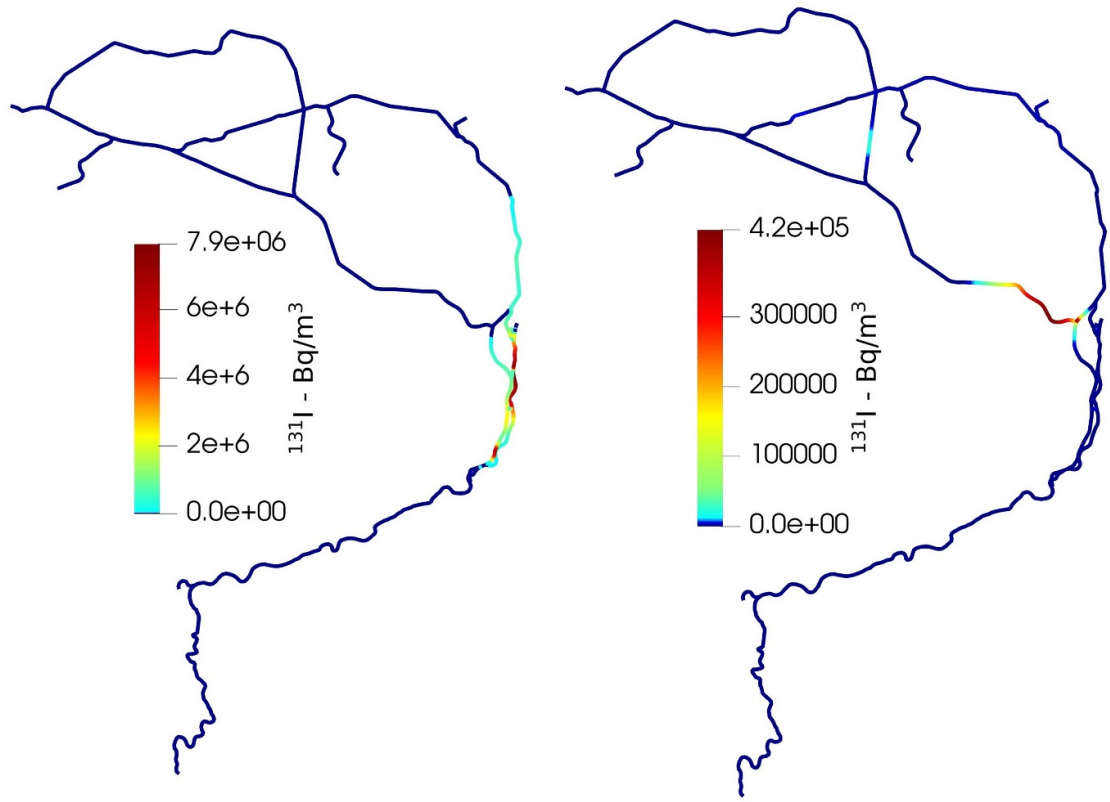

Figure 9. ^{131}I distribution in the Meuse—Campine Canal for low flow scenario after (a) 100 h of initial release (left) and 600 h of initial release (right).

is still higher than the activity concentration of ^{137}Cs. While the contribution to the activity of ^{131}I in the Albert Canal coming from the connecting canals is minimal. Similar results can also be observed in the high flow scenario (figure 10(b)) but with a noticeable influence of the connecting canals (where the spike in activity concentration are visible in figure 10(b); approximately 90 km). This is due to the faster transport of radionuclides and the decreased decay. Although ^{131}I has a considerable impact on the Albert Canal at 7 d, as

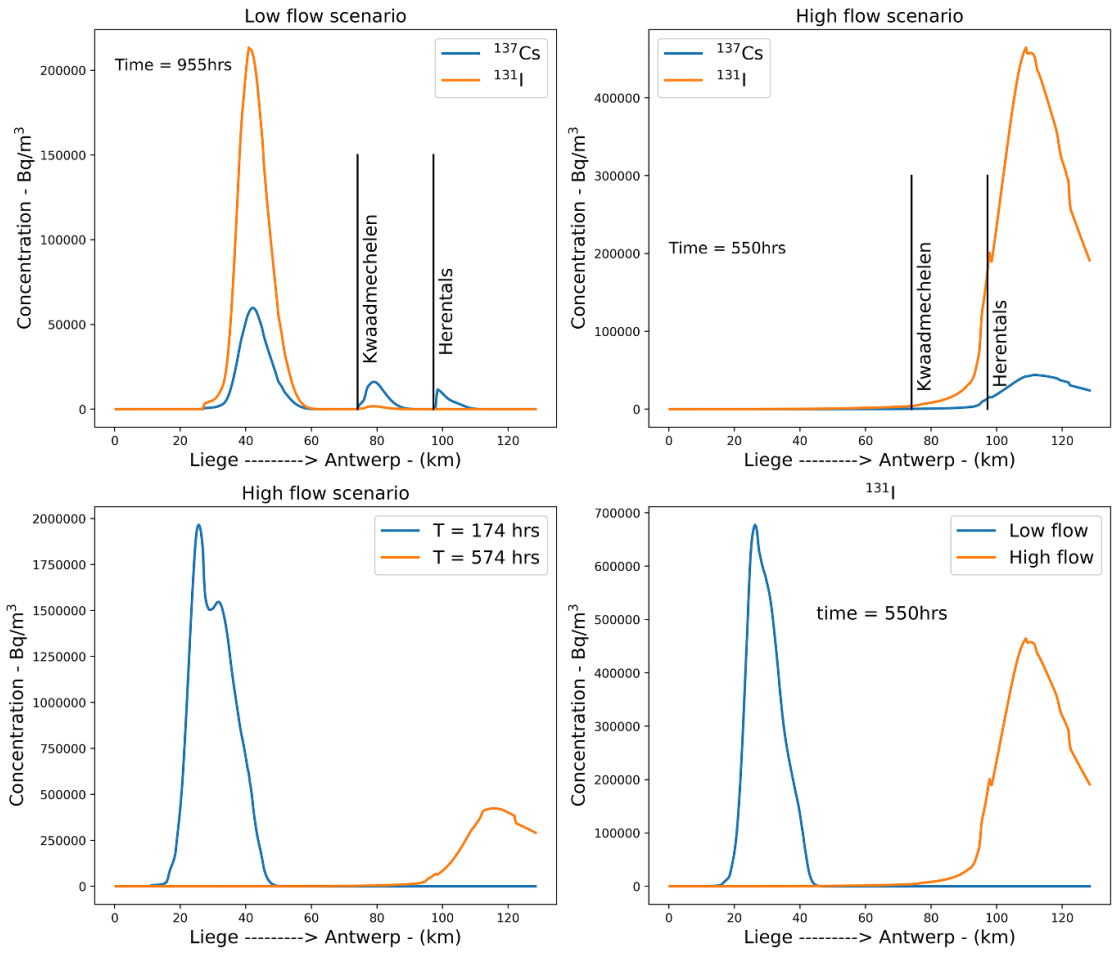

Figure 10. Distribution along the longitudinal profile of the Albert Canal from Liege to Antwerp for (a) comparison of ^{131}I and ^{137}Cs for low flow (top left) (b) comparison of ^{131}I and ^{137}Cs for high flow (top right) (c) ^{131}I distribution after 174 h and 574 h for high flow scenario (bottom left) and (d) ^{131}I distribution for low and high flow after 550 h (bottom right).

seen in figure 10(c), the concentration can drop fourfold within a couple of weeks. After 550 h of the release, the peak concentration is higher for low flows than for the high flow scenario (figure 10(d)). That can be justified by the fact that canals have higher discharge during the high flow scenario (more dilution).

In the case of the Meuse River, the peak ^{131}I concentration at Maastricht is 6.9 and 7 MBq m^{-3} for high and low flows, respectively. Although the arrival time of the plume for high and low flows is similar, there is a significant difference in the passing time of the plume. In the event of high flow, the concentrations remain over 10 000 Bq m^{-3} for around 4 d, whereas in the case of low flow, they remain for about 22 d (figure 11). Even though the ^{131}I decays fast, for low flows the other canal segments (Vise and Lanaye) coming from the Albert Canal into the Meuse River bring additional contamination (figure 11: enlarged area). This is because, in low flow circumstances, radioactive movement in the Albert Canal is exceedingly slow and radioactive plume stays around the bifurcation point for prolonged periods of time. Similarly, we observe the same effects for ^{137}Cs, but they remain below the activity concentration of 10 000 Bq m^{-3}.

3.1.3. Releases from Chooz NPP

The Chooz NPP is located further upstream the Meuse River from the Tihange NPP. Therefore, the deposition of atmospheric releases from Chooz NPP affects wider area. So much so that the release deposition, although less significant, can reach the Zuid Willemsvaart canal (figure 3). Figure 12 shows the ^{131}I and ^{137}Cs distribution on the Meuse River–Canal System after approximately 5 d of release.

After 6 h continuous atmospheric release from Chooz NPP, the affected area in the Meuse River here is clearly larger than that from Tihange NPP. Furthermore, the arrival time (moment when activity is above 10 000 Bq m^{-3} in the water) of the radioactive plume released in the Meuse River at Chooz arrives to Maastricht after 13 h (which is only 2 h later than that observed with Tihange releases). However, the time shift in peak concentration is significant, where it occurs after about 4 d in the case of Tihange and after 10 d in the case of Chooz releases. As a result, due to subsequent ^{131}I decay, the peak concentration in Maastricht

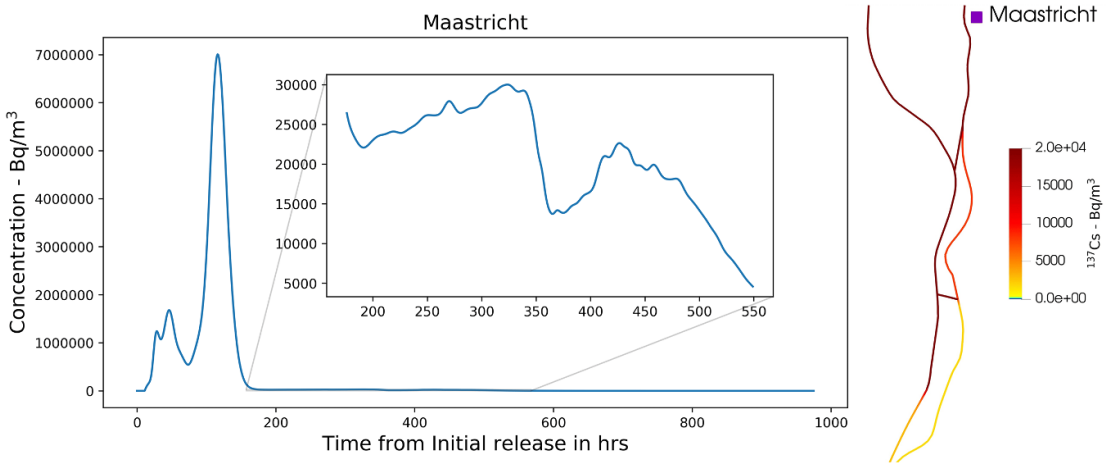

Figure 11. Temporal variation of ^{131}I at Maastricht in the Meuse River and the distribution of ^{131}I at the connection with Albert canal and Meuse River.

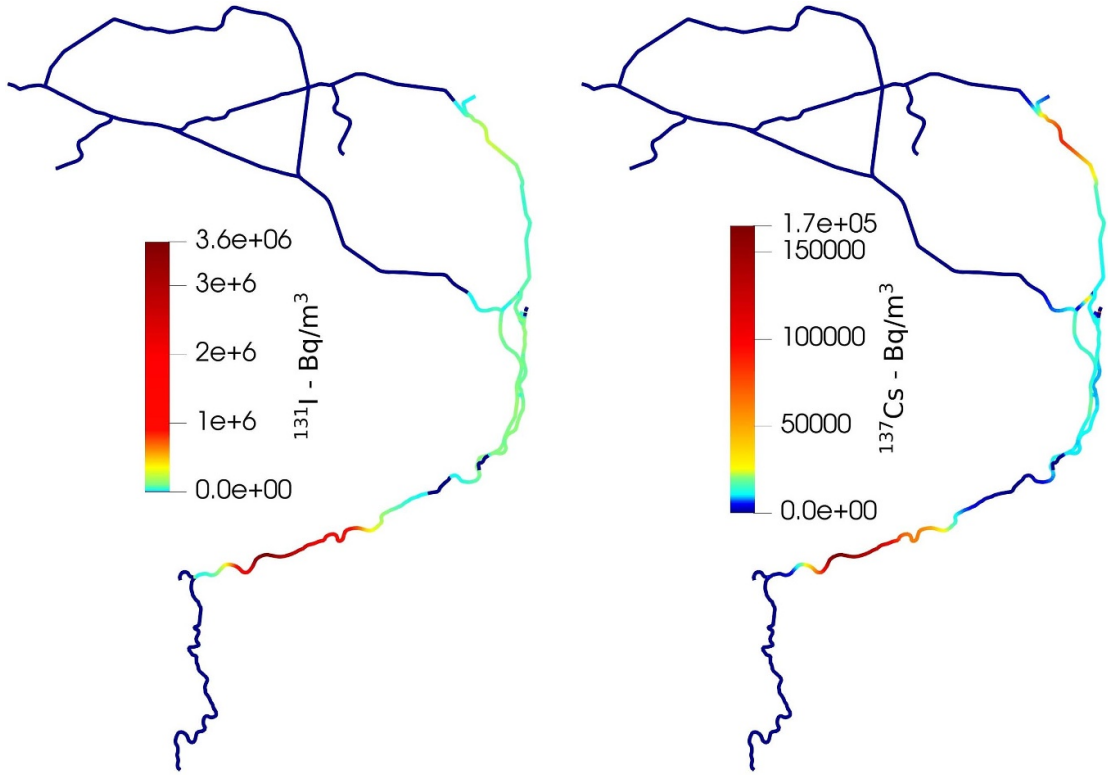

Figure 12. Radioactivity distribution after 125 h in the Meuse—Campine Canal for low flow scenario from Chooz NPP for (a) ^{131}I (left) and (b) ^{137}Cs (right).

is five times lower than that from Tihange releases. In addition, the impact of connecting canals (Vise and Lanaye) from Albert Canal is negligible due to the effect of decay, and thereby, the concentrations in the river remain below 10 000 Bq m^{-3}. Therefore, even if Tihange NPP is located further downstream than Chooz NPP, a longer period of time with activities (^{131}I) above the 10 000 Bq m^{-3} level in Maastricht is observed due to the larger influence of connecting canal as explained in section 3.1.3. Table 4 show the comparison of the arrival, end time and peak concentration (^{131}I) at Maastricht and Liege for both NPPs.

This can be further justified by comparing the results in the Meuse River at Liege, which is located before the connection with the Albert Canal. Here, the residence time is much larger than for the Tihange NPP because of the extent of the plume from the discharge point in the Chooz NPP downstream. Therefore, once the release stops the contaminated water coming from Chooz is still travelling downstream. However, the peak of the release gradually decreases as it moves downstream (table 4). Whereas in the case of the Campine

Table 4. Arrival and End time of the potential plume (^{131}I) in Meuse River and the network of Campine canal at specific location with maximum concentration and time of occurrence at that location.

	City name	Arrival time	End time	Maximum conc. (kBq m^{-3})	Time for max conc. (Hours)
Chooz releases	Liege	12	308	2171	251
	Maastricht	13	367	1317	327
Tihange releases	Liege	2	85	13 333	48
	Maastricht	11	518	7009	115

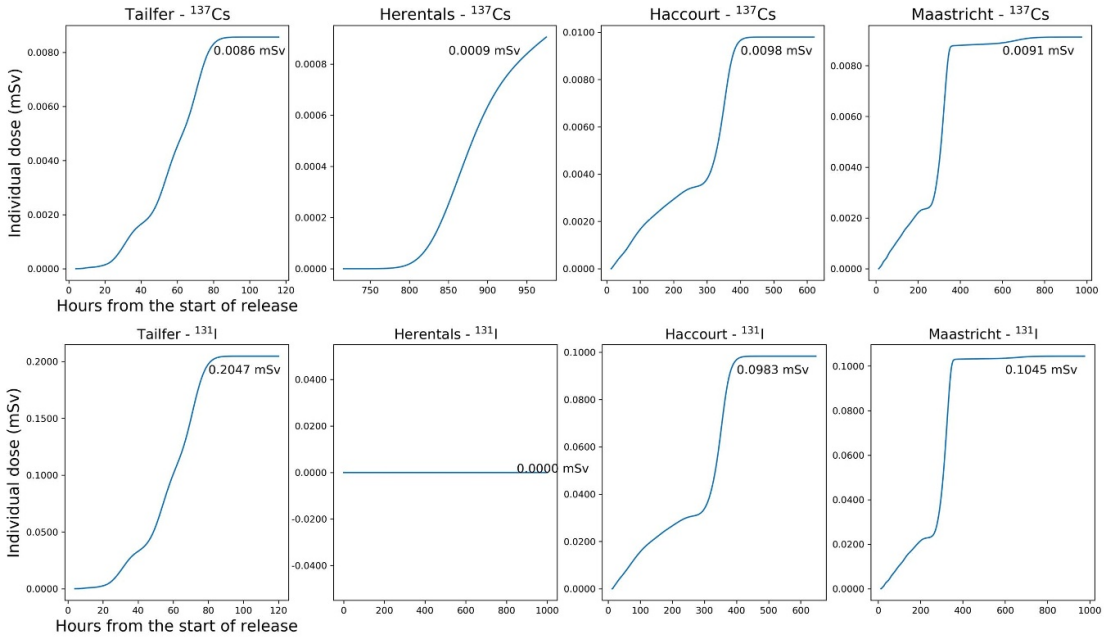

Figure 13. Temporal variation of cumulative Individual dose at drinking water extraction points (Tailfer and Herentals) and hypothetical extraction points (Haccourt and Maastricht) for (a) ^{137}Cs (top) and (b) ^{131}I (bottom): Releases from Chooz NPP.

Canal, as previously observed, the ^{131}I concentrations greatly decline over time, especially in the downstream canals. For example, in the Dessel–Herentals canal at Mol, the peak is about 9 kBq m^{-3} and arrives about a month after the release that persists for about two days. However, the vulnerability of the Albert Canal still remains, with a high concentration of approximately 0.19 MBq m^{-3}, even after a month.

3.2. Dose assessment

To determine the impact of the releases of nuclear power plants in rivers, the dose rate due to ingestion can be used to provide some context to the simulations of activity concentrations. For that, the standard procedure suggested by the ICRP (2007) and ICRP (2020) is followed. Dose limits allowed in Belgium are based on European directives and on the recommendations of international organizations, that stipulates that the total annual dose resulting from the ingestion of drinking water must not exceed 0.1 mSv per year (FANC 2023). This value excludes natural radiation or radiation used for medical purposes. As described in section 2.4, the current water extraction points considered are located at Tailfer in the Meuse River and Herentals in the Albert Canal. It is worth emphasizing that because Tailfer is located upstream from Tihange NPP, the influence of Tihange Nuclear Power Plant is not feasible.

3.2.1. Individual dose

As described earlier, since low flow scenarios have the maximum impact in terms of peak concentration and residence time, they are used to calculate the dose rate. However, the model allows assessment of the impact at any point located on and at the sides of the river. In order to quantify the impact of the radioactive release during low flow scenarios, additional location placed at Haccourt (in the Albert Canal) and Maastricht (in the Meuse River) are also selected to calculate the dose (For location, refer to figure 4). Figure 13 shows the temporal evolution of the cumulative dose and the final dose for releases from Chooz.

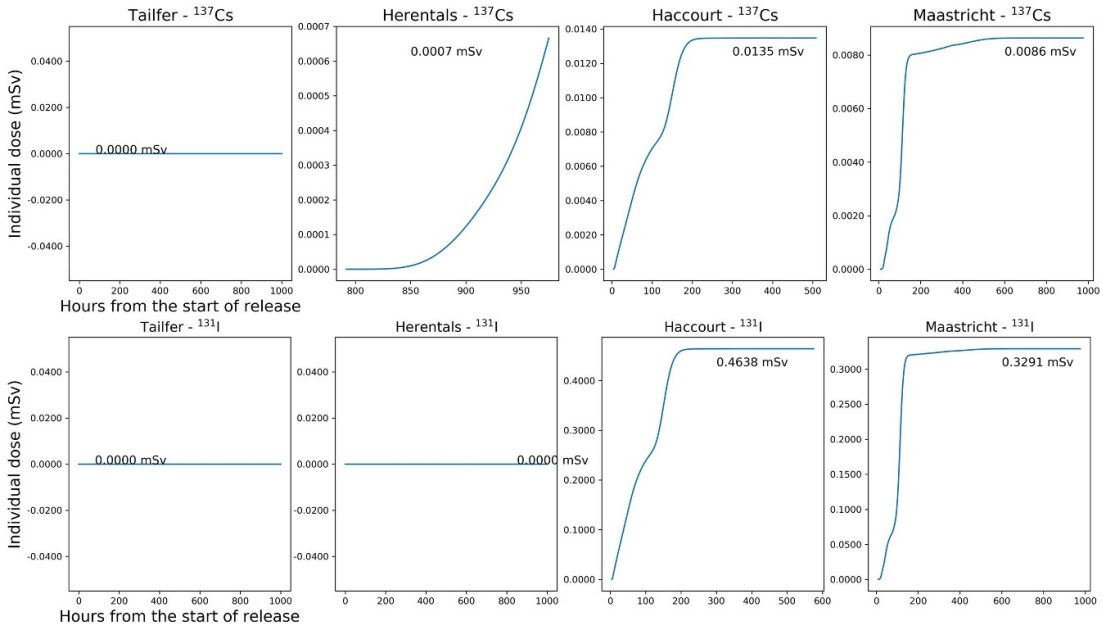

Figure 14. Temporal variation of cumulative Individual dose at drinking water extraction points (Tailfer and Herentals) and hypothetical extraction points (Haccourt and Maastricht) for (a) ^{137}Cs (top) and (b) ^{131}I (bottom): Releases from Tihange Npp.

Figure 13 shows that the cumulative dose of ^{137}Cs in the Meuse River basin and Campine canals is far lower than the permissible limit of 0.1 mSv. Since the low flow scenario in either case does not reach Herentals, the dose here is zero, even for ^{131}I. However, other locations (Tailfer, Haccourt, and Maastricht) have higher individual dose for ^{131}I. The dose rate in the hypothetical locations of Haccourt and Maastricht is close to the 0.1 mSv, but the dose in Tailfer (which provides drinking water to Brussels) is double the permissible limit. This is not the case with ^{137}Cs, as the doses here are comparable (0.0086–0.0098 mSv). This phenomenon, as previously mentioned, is the result of ^{131}I decay. Nonetheless, the results show that the Chooz releases will have significant consequences on the water extraction in Tailfer. Furthermore, the cumulative dose here reaches such level within 3 d, whereas in other locations, the cumulative dose (even if around 0.1 mSv) is reached after about two weeks.

Figure 14 shows temporal evolution of the cumulative dose, and the final dose for releases from Tihange. Herentals (about 100 km from the confluence) show little dose effects, as expected, thus it is safe to conclude that the true impact on drinking water is minimal for releases from Thiange. Again, ^{137}Cs does not exceed 0.1 mSv. However, for ^{131}I, at Haccourt and Maastricht have a considerable influence, with levels three to four times higher than the permissible limits after about 5–7 d. Although, no water extraction occurs at these points, the values can be indicative of heightened vulnerability for individuals from other exposure pathways (such as fish consumption, recreational activities, etc.).

3.2.2. Population dose

The population dose (or collective dose) is calculated from the individual doses estimated for releases from Chooz NPP at Tailfer, which supplies water to the Brussels region. Since individual doses at Herentals (supplies water to Flanders) for releases from both NPPs are exceedingly low, they are not included here. The determination of carcinogenic effects followed by low doses (<0.05 Sv) is based on dose-effect relationships derived from linear no-threshold hypothesis (LNT) (UNSCEAR 2012). The population dose calculated for the consumption of drinking water from Tailfer is 220 Sv in the Brussels region. This corresponds to a 5%–10% increased chance of cancer for 220 people in a 1.2 million population in accordance with the LNT relationship. This indicates that 1 in 6500 people in the Brussels region has an increased chance of risk due to the radiation exposure from drinking water at Tailfer. Furthermore, with a risk of fatal cancer of 0.05 per Sv (ICRP 2007), there will be 12 statistical deaths for an average lifetime risk of about 1×10^{-5} to an individual.

4. Conclusions

The study evaluates the potential impact of radioactive releases at the Chooz and Tihange nuclear power plants on the aquatic systems in the Meuse River basin. An ADD model is developed in order to simulate the transport and dispersion of ^{131}I and ^{137}Cs radioactivity. For this, hypothetical accidents at nuclear power

plants are considered for worst-case contamination scenarios based on past incidents such as Fukushima. The JRODOS atmospheric model is used to obtain the radionuclide fallout in the Meuse River basin. In regard to hydrodynamic conditions, two flow scenarios (low and high flow scenarios) are considered. The results show varying contamination levels in different canals and rivers, with implications for population exposure through drinking water.

Compared to the canal system the radioactivity concentration in the Meuse River declines within days. Notably, radioactive transport in the Albert Canal is slower, particularly in low flow scenarios. Furthermore, in the low flow scenario, it is observed that the radioactive plume from connected canals reached the downstream region of the Albert Canal faster. In general, the low flow scenario had a higher peak concentration and longer residence times for both radionuclides. However, high flows in the Albert Canal cause a shift in flow direction in the Dessel–Kwadmechelan Canal, resulting in recontamination of the Campine Canal after the initial plume has passed. The complex network in and out of Albert Canal has the potential to re-contaminate not just the canals but also the Meuse River, as shown in the case of ^{131}I during low flows.

The distribution of ^{131}I in the Meuse River and Campine Canal varies from that of ^{137}Cs, due to its larger release amount and shorter half-life. Despite the tenfold increase in the initial release of ^{131}I compared to ^{137}Cs, its rapid decay results in substantial reductions in concentration over time. Initial contamination levels for ^{131}I are higher, with peak concentrations around 7.9 MBq m^{-3} after four days, an order of magnitude greater than ^{137}Cs. The faster decay rate of ^{131}I leads to a concentration lower than 10 000 Bq m^{-3} in the Campine Canal within 20–27 d, except for the Albert Canal. The ^{131}I concentrations here remain reasonably high, but no plume from connecting canals can be observed for the low flow scenario due to the longer transport time. Furthermore, the radioactivity concentration in the Albert Canal reduces fourfold within a couple of weeks. The release scenario at Chooz, which is located in the upstream stretch of the river, results in more affected areas in the Meuse River than the Tihange. The initial arrival of radionuclides from Chooz to Maastricht in the Meuse River is delayed compared to Tihange, resulting in lower peak concentrations. However, areas close to Chooz NPP (i.e. in the upstream reach of the river) show significant radioactivity concentrations.

Individual doses are calculated to assess the impact of low flow scenarios on peak concentration and residence time. The study highlights the significant consequences of releases from the Chooz NPP, particularly at Tailfer (which supplies water to the Brussels region), where the dose exceeds the limit of 0.1 mSv. The results show that while the cumulative dose of ^{137}Cs in the Meuse River basin and Campine canals remains below 0.1 mSv, the doses for ^{131}I at hypothetical locations like Haccourt and Maastricht approach this limit. Comparatively, releases from the Tihange NPP show minimal impact on drinking water, with ^{137}Cs levels below this limit, but an impact of ^{131}I at hypothetical sites can be seen.

A future improvement for the model is to use detailed field measurements for radioactivity concentration in order to validate the model and estimate the diffusion coefficients. This validation process would help to ensure that the model is accurately representing the real-world behaviour of radionuclides and would also provide a more precise estimate of diffusion in the canal systems. Additionally, coupled sediment transport and bed evolution models can be beneficial in investigating the deposition and resuspension of sediments, which can also improve the model's accuracy. In this regard, sediment characteristics and concentration measurements will be necessary in order to set up the model that can then be used for long-term studies of the Meuse River basin.

Data availability statement

All data that support the findings of this study are included within the article (and any supplementary files).

Acknowledgment

This research was carried out in the framework of doctoral fellowship PO4500049108, which is awarded to the first author of the present article and is funded by the Engie Electrabel and Belgian Nuclear Research Centre (SCK·CEN). The work was carried out in SCK·CEN and Université catholique de Louvain and the author is thankful for the resources provided. The authors are also grateful to Johan Camps (SCKCEN) for fruitful discussion regarding the scenarios and Katrijn Vandersteen (SCKCEN) for the help in generating simulation results for the atmospheric deposition. The authors are also thankful for members of SLIM team that contributed to the development of the model.

ORCID iDs

Amit Ravindra Patil https://orcid.org/0000-0003-0635-884X
Eric Deleersnijder https://orcid.org/0000-0003-0346-9667

References

Beckers A, Dewals B, Erpicum S, Dujardin S, Detrembleur S, Teller J, Pirotton M and Archambeau P 2013 Contribution of land use changes to future flood damage along the river Meuse in the Walloon region *Nat. Hazards Earth Syst. Sci.* **13** 2301–18

Behrens E, Schwarzkopf F U, Lübbecke J F and Böning C W 2012 Model simulations on the long-term dispersal of ^{137}Cs released into the Pacific Ocean off Fukushima *Environ. Res. Lett.* **7** 034004

Draoui I, Lambrechts J, Legat V, Soares-Frazão S, Hoitink A J F and Deleersnijder E 2020 *Discontinuous Galerkin Method for 1D River Flows* (CRC Press) pp 1114–21

Duffa C *et al* 2016 Development of emergency response tools for accidental radiological contamination of French coastal areas *J. Environ. Radioact.* **151** 487–94

Estournel C *et al* 2012 Assessment of the amount of cesium-137 released into the Pacific Ocean after the Fukushima accident and analysis of its dispersion in Japanese coastal waters *J. Geophys. Res. Oceans* **117** C11014

FANC 2023 *Radiological surveillance of the territory and discharges of class 1 nuclear facilities 2022* Fedral agency for nuclear control Belgium

Goulet R R *et al* 2022 Best practices for predictions of radionuclide activity concentrations and total absorbed dose rates to freshwater organisms exposed to uranium mining/milling *J. Environ. Radioact.* **244–245** 106826

Hofman D *et al* 2011 Computerised decision support systems for the management of freshwater radioecological emergencies: assessment of the state-of-the-art with respect to the experiences and needs of end-users *J. Environ. Radioact.* **102** 119–27

IAEA 2016 *Criteria for Radionuclide Activity Concentrations for Food and Drinking Water (IAEA-TECDOC-1788)* (IAEA)

IAEA 2019 *Modelling of Marine Dispersion and Transfer of Radionuclides Accidentally Released from Land Based Facilities* No. IAEA-TECDOC-1876 (International Atomic Energy Agency)

ICRP 2007 The 2007 recommendations of the International Commission on Radiological Protection ICRP Publication 103 *Ann. ICRP* **37** 2–4

ICRP 2020 Dose coefficients for external exposures to environmental sources *Ann. ICRP* **49** 2

Ievdin I O, Khalchenkov O V, Kovalets I V, Raskob W, Trybushnyi D and Zheleznyak M J 2012 Application of decision support system JRODOS for assessments of atmospheric dispersion and deposition from Fukushima Daiichi nuclear power plant accident *Int. J. Energy Clean Environ.* **13** 179–90

Iwasa Y and Aya S, 1991 Predicting longitudinal dispersion coefficient in openchannel flows *Proc. Int. Symp. on Environmental Hydraulics, (Hong Kong)* pp 505–10

Kovalets I V, Robertson L, Persson C, Didkivska S N, Ievdin I A and Trybushnyi D 2014 Calculation of the far range atmospheric transport of radionuclides after the Fukushima accident with the atmospheric dispersion model MATCH of the JRODOS system *Int. J. Environ. Pollut.* **54** 101–9

Monte L, Boyer P, Brittain J E, Håkanson L, Lepicard S and Smith J T 2005 Review and assessment of models for predicting the migration of radionuclides through rivers *J. Environ. Radioact.* **79** 273–96

Monte L, Brittain J E, Gallego E, Håkanson L, Hofman D and Jiménez A 2009 MOIRA-PLUS: a decision support system for the management of complex fresh water ecosystems contaminated by radionuclides and heavy metals *Comput. Geosci.* **35** 880–96

Monte L, Periañez R, Kivva S, Laptev G, Angeli G, Barros H and Zheleznyak M 2006 Assessment of state-of-the-art models for predicting the remobilisation of radionuclides following the flooding of heavily contaminated areas: the case of Pripyat River floodplain *J. Environ. Radioact.* **88** 267–88

Park S-U, Lee I-H, Joo S J and Ju J-W 2017 Emergency preparedness for the accidental release of radionuclides from the Uljin Nuclear Power Plant in Korea *J. Environ. Radioact.* **180** 90–105

Patil A, Perez F, Lambrechts J, Draoui I and Deleersnijder E, 2022 Numerical modelling of navigable rivers: influence of navigation structures on the Meuse River flow *Proc. 11th Int. Conf. on Fluvial Hydraulics. Presented at the River Flow 2022* (Taylor and Francis) (https://doi.org/10.1201/9781003323037-86)

Periáñez R *et al* 2019 Marine radionuclide transport modelling: recent developments, problems and challenges *Environ. Modelling Softw.* **122** 104523

Raskob W, Landman C and Trybushnyi D 2016 Functions of decision support systems (JRodos as an example): overview and new features and products *Radioprotection* **51** S9–S11

Selivanova A, Hůlka J, Kotík L, Kuča P, Rubovič P, Malátová I, Helebrant J, Koc J, Rulík P and Vlček O 2023 Advanced simulation techniques for the transport of routine atmospheric discharges using the JRODOS system *Prog. Nucl. Energy* **157** 104596

Siclet F, Luck M, Dortz J, Damois C, Ciffroy P, Hendrickx F and Courivaud J-R 2002 Radionuclides concentrations in the Loire river system resulting from routine discharges of five nuclear power plants: assessment of dose to man *Radioprotection* **37** 399–410

Simonsen M, Lind O C, Saetra Ø, Isachsen P E, Teien H-C, Albretsen J and Salbu B 2019 Coastal transport of river-discharged radionuclides: impact of speciation and transformation processes in numerical model simulations *Sc. Total Environ.* **669** 856–71

Tsumune D, Tsubono T, Aoyama M and Hirose K 2012 Distribution of oceanic ^{137}Cs from the Fukushima Dai-ichi Nuclear Power Plant simulated numerically by a regional ocean model *J. Environ. Radioact.* **111** 100–8

Tsuruta H, Oura Y, Ebihara M, Ohara T and Nakajima T 2014 First retrieval of hourly atmospheric radionuclides just after the Fukushima accident by analyzing filter-tapes of operational air pollution monitoring stations *Sci. Rep.* **4** 6717

UNSCEAR 2012 *Sources, Effects and Risks of Ionizing Radiation* (United Nations Scientific Committee on the Effects of Atomic Radiation)

UNSCEAR 2021 Levels and effects of radiation exposure due to the accident at the Fukushima Daiichi Nuclear Power Station: implications of information published since the UNSCEAR 2013 Report (United Nations)

Ward P J, Renssen H, Aerts J C, van Balen R T and Vandenberghe J 2008 Strong increases in flood frequency and discharge of the River Meuse over the late Holocene: impacts of long-term anthropogenic land use change and climate variability *Hydrol. Earth Syst. Sci.* **12** 159–75

Zeng Y and Huai W 2013 Estimation of longitudinal dispersion coefficient in rivers *J. Hydro-environ. Res.* **8** 2–8

Zheleznyak M J 1997 The mathematical modelling of radionuclide transport by surface water flow from the vicinty of the chornobyl nuclear power plant *Condens. Matter Phys.* **12** 37–50

Zheleznyak M J, Demchenko R I, Khursin S L, Kuzmenko Y I, Tkalich P V and Vitiuk N Y 1992 Mathematical modeling of radionuclide dispersion in the Pripyat-Dnieper aquatic system after the Chernobyl accident *Sc. Total Environ.* **112** 89–114